Selective Expansion of Marginal Zone B Cells in Eμ-API2-MALT1 Mice Is Linked to Enhanced IκB Kinase γ Polyubiquitination

Mathijs Baens,[1] Sabine Fevery,[2] Xavier Sagaert,[3] Heidi Noels,[1] Sofie Hagens,[1] Vicky Broeckx,[1] An D. Billiau,[2] Christiane De Wolf-Peeters,[3] and Peter Marynen[1]

[1]Center for Human Genetics, Molecular Genetics, Flanders Interuniversity Institute for Biotechnology, [2]Laboratory of Experimental Transplantation and [3]Division of Morphology and Molecular Pathology, Catholic University of Leuven, Leuven, Belgium

Abstract

The translocation t(11;18)(q21;q21) that generates an API2-MALT1 fusion protein is the most common structural abnormality among the genetic defects reported in mucosa-associated lymphoid tissue (MALT)-type lymphomas, and its presence correlates with the apparent lack of further genetic instability or chromosomal imbalances. Hence, constitutive nuclear factor-κB (NF-κB) activation induced by the API2-MALT1 fusion protein is considered essential for B-cell transformation. To examine its role in B-cell development and lymphomagenesis, Eμ-API2-MALT1 transgenic mice were produced. Our data show that expression of the API2-MALT1 fusion protein alone is not sufficient for the development of lymphoma masses within 50 weeks. Nevertheless, API2-MALT1 expression affected B-cell maturation in the bone marrow and triggered the specific expansion of splenic marginal zone B cells. Polyubiquitination of IκB kinase γ (IKKγ), indicative for enhanced NF-κB activation, was increased in splenic lymphocytes and promoted the survival of B cells *ex vivo*. In addition, we show that the API2-MALT1 fusion resided in the cholesterol- and sphingolipid-enriched membrane microdomains, termed lipid rafts. We provide evidence that association of the MALT1 COOH terminal with the lipid rafts, which is mediated by the API2 portion, is sufficient to trigger NF-κB activation via enhanced polyubiquitination of IKKγ. Taken together, these data support the hypothesis that the API2-MALT1 fusion protein can contribute to MALT lymphoma formation via increased NF-κB activation. (Cancer Res 2006; 66(10): 5270-7)

Introduction

Extranodal marginal zone B-cell lymphoma of mucosa-associated lymphoid tissue (MALT lymphoma) is a rather common type of non–Hodgkin's lymphoma. Three distinct chromosomal translocations have been reported in the pathogenesis: the t(11;18)(q21;q21) results in the expression of an API2-MALT1 fusion protein (1), whereas the t(1;14)(p22;q32) and t(14;18)(q32;q21) inappropriately stimulate expression of *BCL10* and *MALT1*, respectively, by their fusion with the IgH locus of chromosome 14 (2–5). Studies in Bcl10- and Malt1-deficient mice have revealed that both proteins are components of the antigen receptor signaling pathway toward nuclear factor-κB (NF-κB) activation. Bcl10$^{-/-}$ mice are severely immunocompromised due to the failure of their B lymphocytes and T lymphocytes to activate NF-κB and proliferate on antigen binding (6). Similarly, disruption of MALT1 in mice results in defective adaptive immune responses and blocks, depending on the report, T-cell (7) or T-cell receptor (TCR)–induced and B-cell receptor (BCR)–induced NF-κB activation (8).

Both BCL10 and MALT1 play an important role in NF-κB signal transduction; therefore, their overexpression induced by fusion with the IgH enhancer hints at a role for NF-κB deregulation in MALT lymphoma development. Studies in cell lines showed that overexpression of BCL10 activates a NF-κB reporter construct (2, 3), whereas overexpressed MALT1 did not (9, 10). But BCL10 binds to and can dimerize MALT1, and this interaction is essential to synergistically enhance NF-κB activation (10). It was further shown that BCL10 and MALT1 form high molecular weight oligomers that interact with TRAF6 via the COOH terminal of MALT1, which contains two TRAF6-binding sites (11). These BCL10/MALT1 aggregates induce oligomerization of TRAF6, which elicits its E3 ubiquitin ligase activity, resulting in IκB kinase γ (IKKγ; NF-κB essential modulator) polyubiquitination and activation of NF-κB signaling (11). RNA interference experiments further underline the essential role of TRAF6 in NF-κB activation by BCL10 and MALT1 in T lymphocytes (11). In addition, the API2-MALT1 fusion increases polyubiquitination of IKKγ in cell lines and MALT lymphomas and activates NF-κB in this way, a process that depends on the first baculovirus inhibitor of apoptosis repeat (BIR) domain of API2 that mediates oligomerization of the MALT1 COOH terminal (12).

Other studies also attributed an important role to lipid raft membrane microdomains in mediating TCR-induced NF-κB activation (13, 14) and showed CARMA1-mediated recruitment of both BCL10 (15) and MALT1 to the lipid rafts at the TCR on receptor stimulation (16). Failure to recruit BCL10 and MALT1 to the rafts explains the inability of CARMA1-deficient Jurkat T cells to activate NF-κB on TCR engagement (16). In addition, the API2-MALT1 fusion protein was reported to reside in the lipid rafts of human B-cell lymphoma BJAB cells, which was associated with increased constitutive NF-κB activity and resistance to Fas-induced apoptosis (17).

To understand the pathogenic role of the API2-MALT1 fusion protein in MALT lymphoma development, we developed a transgenic mouse model. We show that expression of the API2-MALT1 fusion protein alone is not sufficient for the development of lymphoma masses. However, its expression promotes survival of B cells via enhanced IKKγ polyubiquitination and NF-κB activation and triggers the accumulation of marginal zone B cells. Furthermore, we show an essential role for association of the API2-MALT1 fusion with the lipid rafts in constitutive NF-κB activation.

Note: Supplementary data for this article are available at Cancer Research Online (http://cancerres.aacrjournals.org/).

Requests for reprints: Mathijs Baens, Human Genome Laboratory, Center for Human Genetics, Molecular Genetics, Flanders Interuniversity Institute for Biotechnology, Catholic University of Leuven, Herestraat 49, B-3000 Leuven, Belgium. Phone: 32-16-33-01-30; Fax: 32-16-34-71-66; E-mail: Mathijs.Baens@Med.KULeuven.be.

doi:10.1158/0008-5472.CAN-05-4590

Materials and Methods

Transgene and mice. The open reading frame (ORF) of *API2-MALT1*, representing a fusion between exon 7 of *API2* and exon 8 of *MALT1* (A7M8), was amplified by reverse transcription-PCR (RT-PCR) using Long-Distance PCR (Roche Applied Science, Vilvoorde, Belgium) and cloned into pEμSR (18), a gift of Dr. Suzanne Cory (The Walter and Eliza Hall Institute of Medical Research, Victoria, Australia). The pEμSR-A7M8 construct was digested by *Not*I to release the transgene, which was gel purified (QIAquick Gel Extraction, Qiagen Benelux BV, Venlo, the Netherlands) before injection into fertilized eggs. Transgenic FVB mice were generated by pronuclear microinjection as described previously (19) and identified by PCR analysis of tail DNA. Two transgenic strains, AM31 and AM37, were bred and maintained at the experimental animal facility of the Catholic University of Leuven (Leuven, Belgium) under non-pathogen-free conditions. All animal experiments were done in accordance with institutional guidelines.

Histology and immunohistochemistry. Groups of five mice of both strains were sacrificed at ages 5, 10, 15, 20, 30, 40, and 50 weeks, and the macroscopic findings as well as microscopic features of the spleen, thymus, bone marrow, lymph nodes, stomach, intestines, lung, and salivary glands were compared with those of their wild-type (WT) FVB littermates. Biopsies from all organs were fixed in formalin and B5 and embedded in paraffin. H&E-stained sections (4 μmol/L) were examined blindly for the presence of histopathologic lesions. Parts of the stomach, thymus, and spleen were frozen in liquid nitrogen and kept at −80°C until use. Biopsies of the femur were B5 fixed and decalcified overnight in formic acid (10%) before paraffin embedding.

Paraffin sections (4 μm) of the spleen were immunostained with BCL10 (goat polyclonal α-mouse antibody, Santa Cruz Biotechnology, Inc., Tebu-bio, Boechout, Belgium). Deparaffinized slides were immersed in citrate buffer (pH 6) and placed in a warm water bath (95-99°C) for 40 minutes to do epitope retrieval. Following incubation with the primary antibody (30 minutes at room temperature), slides were incubated for 30 minutes at room temperature with biotin-labeled rabbit α-goat Ig (Dako Belgium NV, Heverlee, Belgium). The third step consisted of incubation with the avidin-biotin complex method visualization system, also from Dako.

Flow cytometric analyses. Single-cell suspensions of bone marrow and spleen were labeled with FITC-, phycoerythrin-, or PerCP-conjugated antibodies (BD Biosciences, Erembodegem, Belgium) reactive to CD3, CD21, CD23, CD40, B220, sIgM, and sIgD. Stained cells were analyzed with a FACSort (BD Biosciences) using the CellQuest software.

Constructs. The plasmid pcDNA3.1 with a NH_2-terminal Flag-tag or HA-tag was used to generate the expression constructs for the API2-MALT1 fusion [pcD-F-A7M8, pcD-F-A7M8-ΔC80 (AA 1-848), pcD-F-A7M8-ΔB1 (AA 103-946), and pcD-F-A7M8-E928A], MALT1 (pcD-F-MALT1) and AA 505-824 of MALT1 (pcD-F-MALT1-Cter), IKKγ (pcD-F-IKKγ), and ubiquitin (pcD-HA-Ub). The ORFs of A7M8, MALT1, MALT1-Cter, IKKγ, and ubiquitin were amplified by RT-PCR using Long-Distance PCR. An oligonucleotide linker encoding the myristoylation-palmitoylation motif of the Lck kinase (MGCVCSSNPEDD) was inserted upstream of the flag epitope to generate pcD-mp-F-MALT1-Cter. The expression construct for A20 (pCAGGS-E-A20) was a generous gift of Dr. Rudi Beyaert (Department of Molecular Biomedical Research, Ghent, Belgium) (20).

Cell culture and NF-κB reporter assays. HEK293T cells were cultured in DMEM-F12 (N.V. Invitrogen, Merelbeke, Belgium) supplemented with 10% FCS at 37°C in 5% CO_2. HEK293T cells (5×10^5) were transfected with 1 μg DNA containing 20 ng NF-κB luciferase reporter construct (pIgκ3ConALuc) and 20 ng β-galactosidase expression vector (pEL1-β-gal), a mixture of the expression constructs to test (2-200 ng) and the appropriate empty parental expression vector to keep the total amount of DNA at 1 μg/well of a six-well plate using GeneJuice Transfection Reagent (Novagen, VWR International, Haasrode, Belgium). Twenty-four hours after transfection, cells were harvested in 1× PBS and lysed in 30 μL Passive lysis buffer (Promega Benelux BV, Leiden, the Netherlands). Cell lysate (3 μL) was assayed for luciferase and β-galactosidase activities using a FLUOstar Galaxy Plate Reader (BMG Labtechnologies GmbH, Offenburg, Germany). Fold NF-κB stimulation was calculated by dividing the luciferase activity, normalized to β-galactosidase activity for each sample, by that observed in the control containing only empty expression vector.

Western blot analysis and immunoprecipitations. Cell suspensions from spleens of WT and AM31 mice were depleted from erythrocytes with red cell lysis buffer (Erythrocyte Lysis Buffer, Qiagen Benelux BV) and washed with 1 mL ice-cold PBS, and a 40-μm cell strainer (BD Biosciences) was used to separate mononuclear cells. B cells and T cells were isolated from these single-cell suspensions by negative selection using the Mouse B Cell or Pan T Cell Isolation kits (Miltenyibiotech, Utrecht, the Netherlands) according to the manufacturer's instructions, which were lysed for 30 minutes on ice in 1% Triton X-100, 50 mmol/L Tris-Cl (pH 7.4), 300 mmol/L NaCl, and 5 mmol/L EDTA supplemented with 1× Complete protease inhibitor cocktail (Roche Applied Science). Following removal of debris by centrifugation at 13,000 rpm for 10 minutes at 4°C, cell lysates were fractionated on 4% to 12% (NuPAGE, N.V. Invitrogen) or 15% SDS-polyacrylamide gels and transferred to polyvinylidene difluoride membranes (Amersham Biosciences Benelux, Roosendaal, the Netherlands). Immunoblotting for API2-MALT1 (A7M8) was conducted with a rabbit polyclonal antiserum raised against the COOH terminal (AA 731-824) of MALT1 (α-MALT1-Cter).

For the detection of IKKγ polyubiquitination, lysates from HEK293T cells transfected with pcD-F-IKKγ /pcD-HA-Ub and pcD-F-A7M8, pcD-F-A7M8-ΔC80, pcD-F-A7M8-ΔB1, pcD-F-MALT1-Cter, pcD-mp-F-MALT1-Cter, or empty vector were precleared with protein G-Sepharose (Amersham Biosciences Benelux) for 2 hours before immunoprecipitation overnight with an antibody against IKKγ (FL-419, Santa Cruz Biotechnology). Immunoprecipitates were washed four times in lysis buffer, resolved by SDS-PAGE, and detected with α-HA (12CA5, Roche Applied Science), α-Flag (Sigma-Aldrich NV, Bornem, Belgium), or α-E-tag (Amersham Biosciences Benelux). IKKγ immunoprecipitated from isolated murine lymphocytes was detected with a mouse monoclonal α-IKKγ antibody (B3, Santa Cruz Biotechnology).

Purification of lipid raft membrane fractions. Single-cell suspensions of spleens were prepared as described above; splenocytes (30×10^6) or HEK293T cells (15×10^6) transfected with A7M8, MALT1, or mp-MALT1-Cter were washed with ice-cold 1× PBS and lysed in 2 mL TMN lysis buffer [1% Triton X-100, 25 mmol/L 2-(*N*-morpholino)ethanesulfonic acid, and 150 mmol/L NaCl] supplemented with 1× Complete protease inhibitor cocktail. Two milliliters of an 80% sucrose solution in 1× TMN was mixed with the lysate, and this was overlaid with 4 mL of 30% sucrose in 1× TMN followed by 4 mL of a 5% sucrose solution in 1× TMN. The samples were centrifuged in a SW41 rotor (Beckman Coulter, Analis SA, Namur, Belgium) at 38,000 rpm overnight at 4°C. Fractions (1 mL) were taken from the top of the gradient, of which 300 μL (fractions 1-8) or 100 μL (fractions 9-12) were concentrated via $CHCl_3$/methanol precipitation, resuspended in 1× SDS gel loading buffer, and subjected to SDS-PAGE and Western blotting with α-MALT1-Cter and α-Lyn (44) (Santa Cruz Biotechnology) antibodies. The lactate dehydrogenase activity of each fraction (50 μL) was assessed (CytoTox-ONE Solution kit, Promega Benelux BV) to evaluate contamination of the raft fractions with cytosolic proteins (Supplementary Table S1).

Preparation of bone marrow cells and *in vitro* colony assays. Single-cell suspensions of bone marrow were prepared by repeatedly flushing the cells from femurs with RPMI 1640 (N.V. Invitrogen), and mononuclear cells were isolated via filtration (40 μm cell strainer). Colony-forming unit pre-B cells were assayed by suspending 10^5 mononuclear cells in 1 mL aliquots of MethoCult M 3630 medium (StemCell Technologies, Inc., Vancouver, British Columbia, Canada) supplemented with recombinant interleukin-7 (IL-7) in 35-mm plastic Petri dishes. Femoral bone marrow cells from three mice per group were assayed each in duplicate, and colonies were scored on day 10 of culture.

B-cell survival assay. $CD19^+$ B cells were isolated from single-cell suspensions of spleen by positive selection with CD19 microbeads (Miltenyibiotech) according to the manufacturer's instructions and cultured in 24-well plates (10^6 in 0.5 mL) in RPMI containing 10% FCS and 50 μmol/L 2-mercaptoethanol. Cells were harvested after 4 and 5 days of culture, and the number of viable cells was determined via trypan blue exclusion using a Vi-Cell XR Cell Viability Analyzer (Beckman Coulter).

Results

Generation of API2-MALT1 transgenic mice. To examine the role of the API2-MALT1 fusion protein in MALT-type lymphoma development, we generated transgenic mice in which an API2-MALT1 fusion was expressed throughout B-cell lymphopoiesis. We chose to express the *API2-MALT1* fusion gene identified previously in a case of MALT-type lymphoma and that represents a fusion between exon 7 of *API2* and exon 8 of *MALT1* (1). The resulting A7M8 fusion protein contains the three BIR domains of API2 fused to the caspase p20-like domain and the TRAF6 interaction motifs (11) of MALT1 (Fig. 1*A*) and is representative for 50% of all reported cases (21). We used the pEμSR vector with the Ig intronic heavy chain enhancer (Eμ) as regulatory element, which allows high-level specific expression in lymphoid cells (18) and is already active in the earliest committed B lymphocyte progenitors (pre-pro-B cells) when D_H to J_H rearrangement first takes place (22).

The EμSR-A7M8 transgene, released via a *Not*I digestion, was injected into FVB mouse zygote pronuclei using standard techniques, and two transgenic FVB strains were bred, AM31 and AM37. Western blot quantification (Image Station 440, Kodak NV, Zaventem, Belgium) showed that the API2-MALT1 expression level in splenic lymphocytes was equal to endogenous MALT1 for strain AM37, whereas its expression was 4-fold higher in line AM31 (Fig. 1*B*). Western blots also confirmed that the Eμ enhancer drives expression of API2-MALT1 in both B lymphocytes and T lymphocytes of AM31 transgenic mice (Fig. 1*C*). API2-MALT1 transgenic animals were viable, fertile, and seemed healthy with no overt abnormalities detected at autopsy.

Morphology and immunohistochemistry. As no manifest abnormalities could be detected in transgenic mice at autopsy, we did a detailed histologic examination. Groups of five mice of both lines (AM31 and AM37) were sacrificed at ages 5, 10, 15, 20, 30, 40, and 50 weeks, and the histologic features of the spleen, thymus, bone marrow, lymph nodes, stomach, intestines, lung, and salivary glands were compared with those of their WT FVB littermates. No histologic signs of spontaneous lymphoma development could be found after 50 weeks of observation for both transgenic strains. Moreover, no macroscopic or microscopic differences were noted in any of the organs examined during aging, except for some differences found in the spleen of AM31 transgenic mice: in these animals, nicely formed germinal centers were already developed at age 5 weeks, although they could not be identified before age 10 weeks in their WT littermates (data not shown). At age ≥10 weeks, these germinal centers were larger, the marginal sinus was more prominent, and the follicle mantle, comprising the lymphocytic corona and the marginal zone, tended to be larger in AM31 transgenic mice compared with their WT littermates of the same age (Fig. 2*A* and *B*).

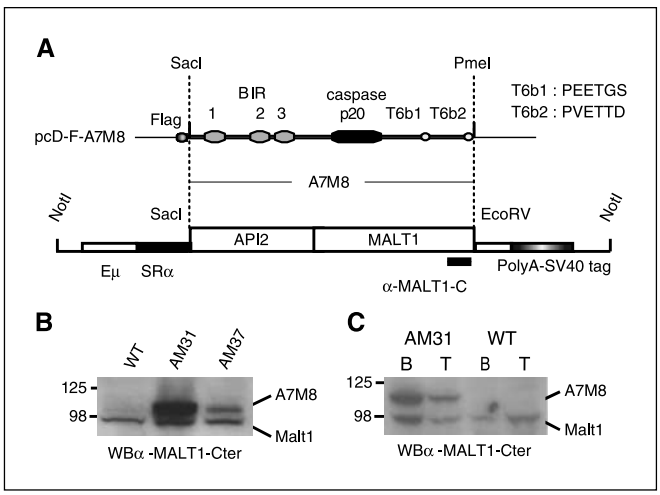

Figure 1. Generation of API2-MALT1 transgenic mice. *A,* the API2-MALT1 cDNA (*A7M8*) represents a fusion between exon 7 of *API2* and exon 8 of *MALT1*, resulting in the fusion of the three BIR domains of API2 to the caspase p20-like domain and the two TRAF6-binding sites of MALT1 (*T6b1* and *T6b2*). *White and black boxes,* A7M8 cDNA was inserted 3′ of the Eμ/SRa enhancer/promoter, driving high-level specific expression in lymphoid cells. *Underlined,* COOH terminal of MALT1 (AA 731-824) recognized by the rabbit polyclonal α-MALT1-Cter (α-*MALT1-C*). *B,* Western blot analysis (*WB*) of cellular extracts from splenic lymphocytes from FVB WT mice and AM31 and AM37 transgenic mice. *C,* Western blot analysis of purified B lymphocytes (*B*) and T lymphocytes (*T*) from AM31 transgenic and FVB WT mice. Blots were detected with the α-MALT1-Cter antibody. A7M8 protein and endogenous Malt1. Protein sizes are in kDa.

A common feature of t(11;18) and t(1;14) MALT lymphomas is nuclear localization of BCL10 (23–26). Staining for the BCL10 protein revealed diffuse cytoplasmic expression of BCL10 in the B cells of the follicle mantle with, in between, a very few scattered B cells showing nuclear staining. However, no difference in staining pattern was noted between AM31 and WT animals (data not shown).

API2-MALT1 affects B-cell maturation and survival. We next analyzed an effect of API2-MALT1 expression on the development and maturation of haematopoietic cells via flow cytometric analyses. Whereas expression of CD3 and B220 on splenic lymphocytes was comparable between 12-week-old WT and AM31 mice (Fig. 3*A*), examination of $B220^+$ lymphocytes showed that the $IgM^{high}IgD^{low}$ and $CD21^{high}CD23^{low}$ subsets corresponding to the marginal zone B-cell population were increased in AM31 mice (Fig. 3*B* and *C*), consistent with the morphologic findings of an enlarged marginal zone B-cell area (Fig. 2*A*). To assess a possible effect of API2-MALT1 on survival of B cells, $CD19^+$ B cells were isolated from mouse spleens and cultured *in vitro*. B cells isolated from AM31 mice were found to have a greater *in vitro* survival capacity than those from control littermates (Fig. 3*D*). Besides an effect on the marginal zone B-cell subset, there was also a specific increase of the $IgM^{low}IgD^{low}$ (naive) B-cell population in AM31 mice (Fig. 3*C*). The above-mentioned effects were also apparent in 8- and 20-week-old AM31 mice (data not shown), suggesting that API2-MALT1 expression *in vivo* favors the survival of splenic marginal zone B cells.

Fluorescence-activated cell sorting (FACS) profiles of bone marrow cells revealed impaired T-cell and B-cell populations ($CD3^+/B220^+$) in AM31 mice compared with their WT littermates (Fig. 4*A*), with a clear decrease of the number of pre-B/naive B cells ($CD40^+B220^+$) and naive B cells ($sIgM^+B220^+$; Fig. 4*B* and *C*). Furthermore, pre-B cells from AM31 mice failed to form colonies in methylcellulose containing IL-7 (Fig. 4*D*), which could not be counteracted by extending the culture period.

API2-MALT1 enhances IKKγ polyubiquitination and is associated with the lipid rafts. The above-mentioned effects in the AM31 mice might be explained by the activation of the NF-κB pathway by API2-MALT1 (9, 10). The transcription factor NF-κB plays a critical role in the survival of resting B cells as mice, deficient for any of the five NF-κB proteins, have reduced numbers of peripheral (especially marginal zone) B cells (27). Western blot analysis of IKKγ immunoprecipitates from splenic lymphocytes indeed showed enhanced polyubiquitination of IKKγ caused by API2-MALT1 expression (Fig. 5*A*), indicative for NF-κB activation

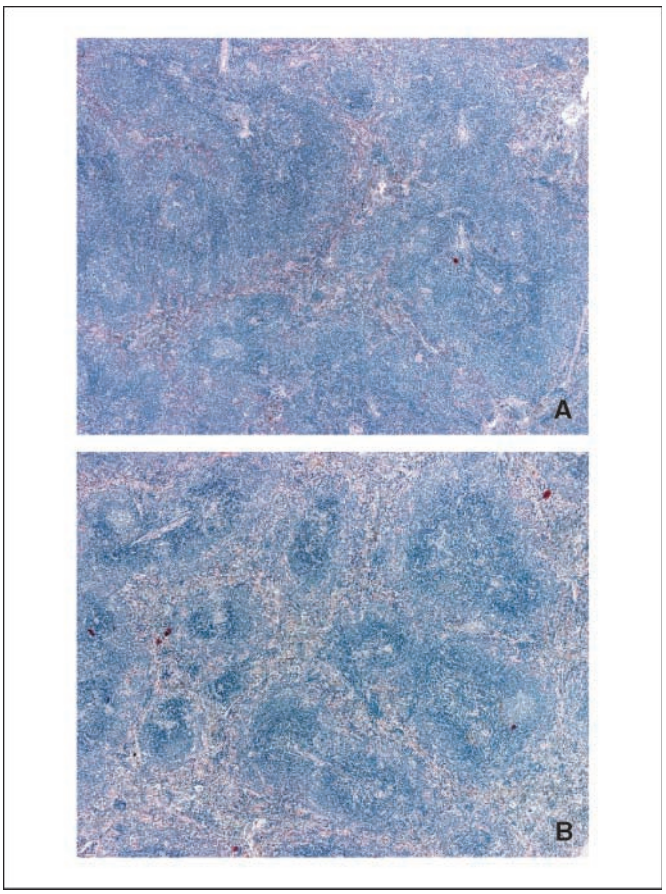

Figure 2. Spleen morphology of API2-MALT1 transgenic mice and WT littermates at age 20 weeks. AM31 mice show a reduction of red pulpa with an increase of white pulpa due to an expanded marginal zone (*A*) compared with their WT littermates (*B*).

and consistent with the increased levels of IKKγ polyubiquitination observed in MALT lymphomas (12). These data suggest that API2-MALT1 expressing B cells preferentially accumulate *in vivo* due to an inherent survival advantage caused by increased NF-κB activity.

A recent report further indicated an essential role for lipid raft association of MALT1 in TCR-induced NF-κB activation (16). Purification of detergent-resistant membrane (DRM) complexes from lymphocytes of AM31 mice showed that API2-MALT1 resided in the lipid rafts, in contrast to endogenous MALT1, which was detected only in the cytosolic fractions (Fig. 5*B*). Its presence in the raft fractions was not due to a cytosolic contamination in view of the negligible lactate dehydrogenase activities of these fractions (Supplementary Table S1). Therefore, these data suggest that permanent association of API2-MALT1 with the raft membrane fractions might represent a mechanism for constitutive NF-κB activity.

Raft association of MALT1-Cter triggers IKKγ polyubiquitination and NF-κB activation. To investigate a possible link between raft association and NF-κB activation by API2-MALT1, we isolated DRM complexes from HEK293T cells transiently expressing A7M8. NF-κB activation by API2-MALT1 was associated with enhanced total cellular and IKKγ polyubiquitination (Fig. 6*C*) and with its lipid raft localization (Fig. 6*B*), which was not due to a cytosolic contamination (Supplementary Table S1). To further explore the mechanism by which API2-MALT1 associates with the lipid rafts, we generated A7M8 deletion constructs (Fig. 6*A*). Deletion of the first BIR domain of A7M8 abolished its potential to induce IKKγ polyubiquitination and activate a NF-κB reporter in HEK293T cells (Fig. 6*C*) consistent with a recent report (12). This deletion, however, also prevented the association of A7M8-ΔB1 with the lipid rafts (Fig. 6*B*). Treatment of the cells with increasing concentrations of methyl-β-cyclodextrin, which disrupts lipid rafts by specific cholesterol depletion, reduced the potential of the A7M8 fusion to activate the NF-κB reporter, whereas the overall expression levels of A7M8 were unaffected (Supplementary Fig. S1A), further strengthening the link between raft association of API2-MALT1 and NF-κB activation. In contrast, deletion of the second TRAF6-binding site (A7M8-ΔC80) did not affect its association with the lipid rafts (Fig. 6*B*), yet this construct was

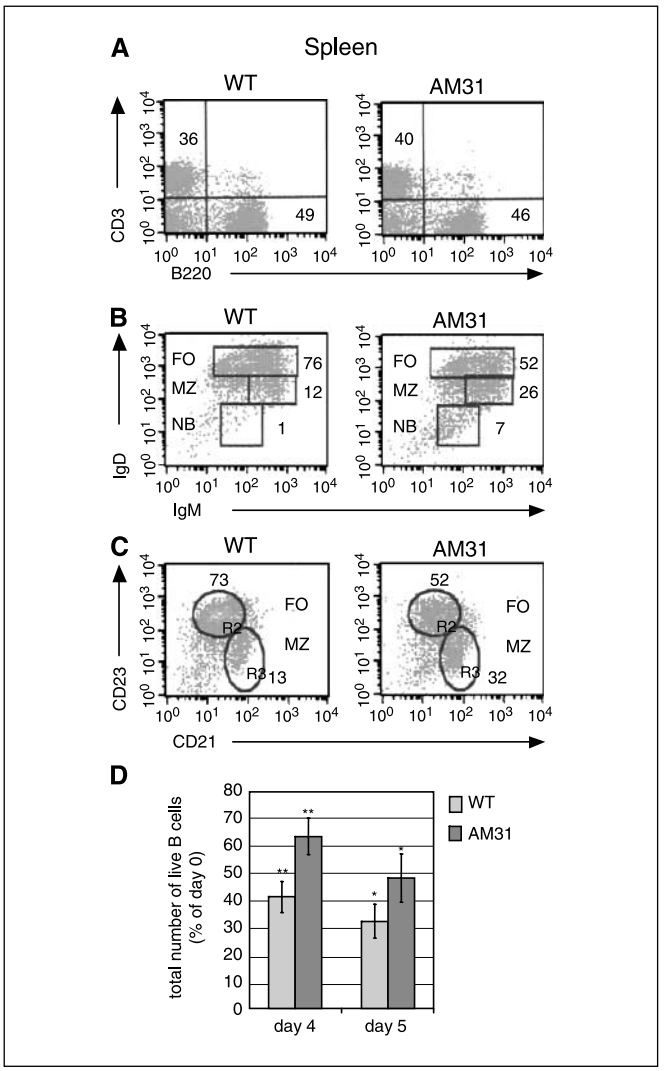

Figure 3. API2-MALT1 promotes B-cell survival. FACS analyses for splenic B cells from 12-week-old WT and AM31 mice labeled with the indicated antibodies. Percentages of positive cells. *A*, B-cell and T-cell populations ($CD3^+/B220^+$) in spleen (lymphocyte gate). *B*, surface IgM/IgD. *FO,* follicular B cells; *MZ,* marginal zone B cells; *NB,* naive B cells. *C*, CD21/CD23 expression on B220-gated splenic B lymphocytes. Representative data of one experiment. *D*, splenic $CD19^+$ B cells from AM31 or WT mice were cultured *in vitro*, and the number of surviving B cells was expressed as a proportion of the number present at day 0. *Columns,* mean values from four mice (12 weeks) of each group; bars, SD. $P = 0.0012$ and $P = 0.013$ at days 4 and 5, respectively.

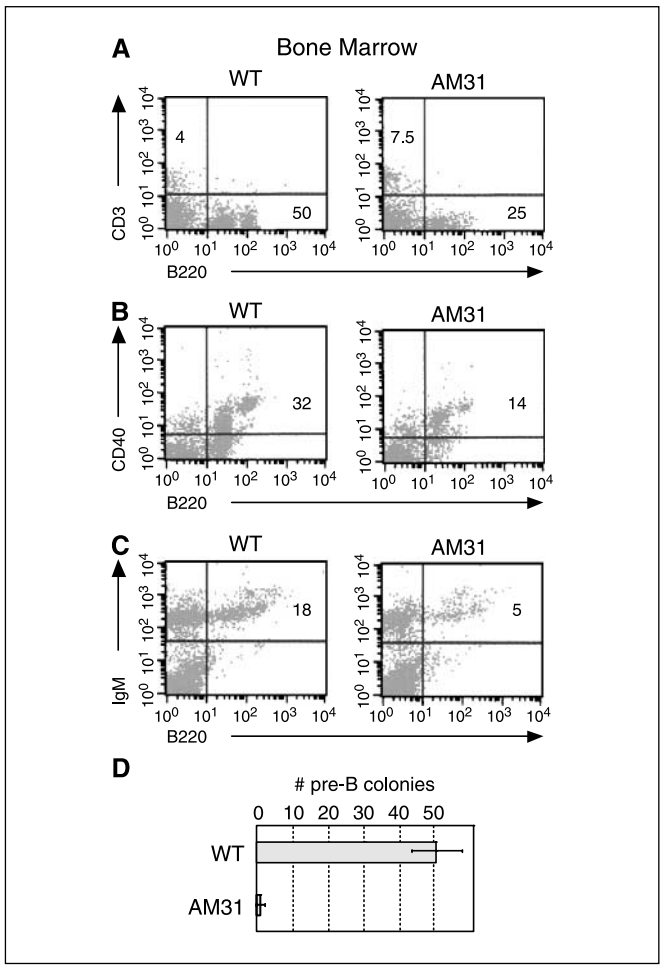

Figure 4. API2-MALT1 affects B-cell maturation in the bone marrow. FACS analyses for bone marrow cells from 12-week-old WT and AM31 mice. *A*, B-cell and T-cell populations ($CD3^+/B220^+$). *B*, number of pre-B/naive B cells ($CD40^+B220^+$). *C*, naive B cells ($sIgM^+B220^+$) in bone marrow cells (lymphocyte gate). Representative data of one experiment. *D*, pre-B colony formation from bone marrow cells of WT and AM31 mice.

completely defective for IKKγ polyubiquitination and NF-κB activation (Fig. 6*C*). Likewise, mutation of the second TRAF6-binding site (A7M8-E928A) was sufficient to abolish NF-κB signaling (Supplementary Fig. S1B). This suggests that raft association precedes TRAF6-mediated polyubiquitination of IKKγ. The importance of this ubiquitination for NF-κB activation by A7M8 was shown by coexpression of the deubiquitinating enzyme A20, which efficiently suppressed A7M8-induced ubiquitination and NF-κB activation in HEK293T cells (Fig. 6*C*).

In contrast to API2-MALT1, expression of MALT1 does not activate NF-κB signaling in HEK293T cells (10), and purification of DRM complexes showed that MALT1 is not associated with the lipid rafts in HEK293T cells (Fig. 6*B*). To prove that raft association of the MALT1 COOH terminal is sufficient to enhance IKKγ polyubiquitination and NF-κB signaling, we generated a cDNA encoding the myristoylation-palmitoylation signal from Lck linked to residues 505-824 of MALT1 (mp-MALT1-Cter). Western blot analysis of purified DRM complexes confirmed that mp-MALT1-Cter resided in the rafts (Fig. 6*B*), which coincided with NF-κB activation and IKKγ polyubiquitination, whereas MALT1-Cter failed to do so (Fig. 6*C*). Altogether, these data indicate that the first BIR domain of API2 triggers NF-κB activation by API2-MALT1 via raft association of the COOH terminal of MALT1, which is essential for TRAF6-mediated polyubiquitination of IKKγ.

Discussion

To understand the pathogenic role of the t(11;18) translocation in MALT-type lymphomas, we produced and characterized a transgenic FVB mouse strain (AM31), in which the API2-MALT1 transcript was expressed throughout B-cell lymphopoiesis. No morphologic signs of spontaneous (MALT-type) lymphoma development could be found in the API2-MALT1 transgenic mice after 50 weeks of observation. This finding suggests that the t(11;18)(q21;q21) may not be sufficient to induce lymphoma masses despite the fact that this translocation occurs as a sole anomaly in MALT-type lymphomas. This observation is in line with the hypothesis that MALT-type lymphomagenesis is a multistep process in which other additional environmental and microbial or (still unknown) host genetic factors play a pivotal role besides the t(11;18)(q21;q21) (28). Alternatively, the observation period of 1 year may not be sufficient for an indolent lymphoma to develop. Other transgenic mouse models for small B-cell non–Hodgkin's lymphomas with a similar indolent clinical behavior, such as t(14;18)(q32;q21)-associated follicular lymphoma, only developed lymphomas at low incidence (3-15%) after 2 years of observation (29).

A striking feature of MALT-type lymphomas with t(1;14)(p22;q32) or t(11;18)(q21;q21) is an unusual nuclear localization of BCL10 (23–26). Recent data support a role for MALT1 in the nucleocytoplasmic shuttling of BCL10 (30). Overexpression of BCL10 induced by the t(1;14) might cause less efficient export of BCL10 resulting in its nuclear retention. Indeed, BCL10 was shown to be expressed at high levels in the nuclei of splenic marginal zone B cells in transgenic mice, in which BCL10 expression is driven by Ig enhancers (31). As a result of the t(11;18), MALT1 protein levels are expected to be reduced by half as the translocated allele expresses API2-MALT1.

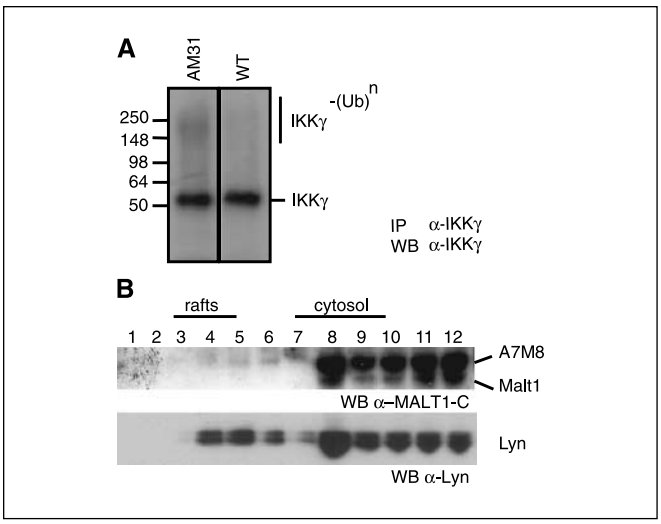

Figure 5. API2-MALT1 promotes IKKγ polyubiquitination and associates with lipid rafts in AM31 mice. *A*, IKKγ was immunoprecipitated (*IP*) from splenic lymphocytes with a rabbit polyclonal α-IKKγ antibody (FI-419). Polyubiquitination of IKKγ was determined by immunoblotting with a mouse monoclonal α-IKKγ antibody (B3). $IKK\gamma^{-(Ub)n}$, polyubiquitinated IKKγ. *B*, lysates of splenic lymphocytes were subjected to sucrose density gradient centrifugation, and fractions were immunoblotted with α-MALT1-Cter and α-Lyn.

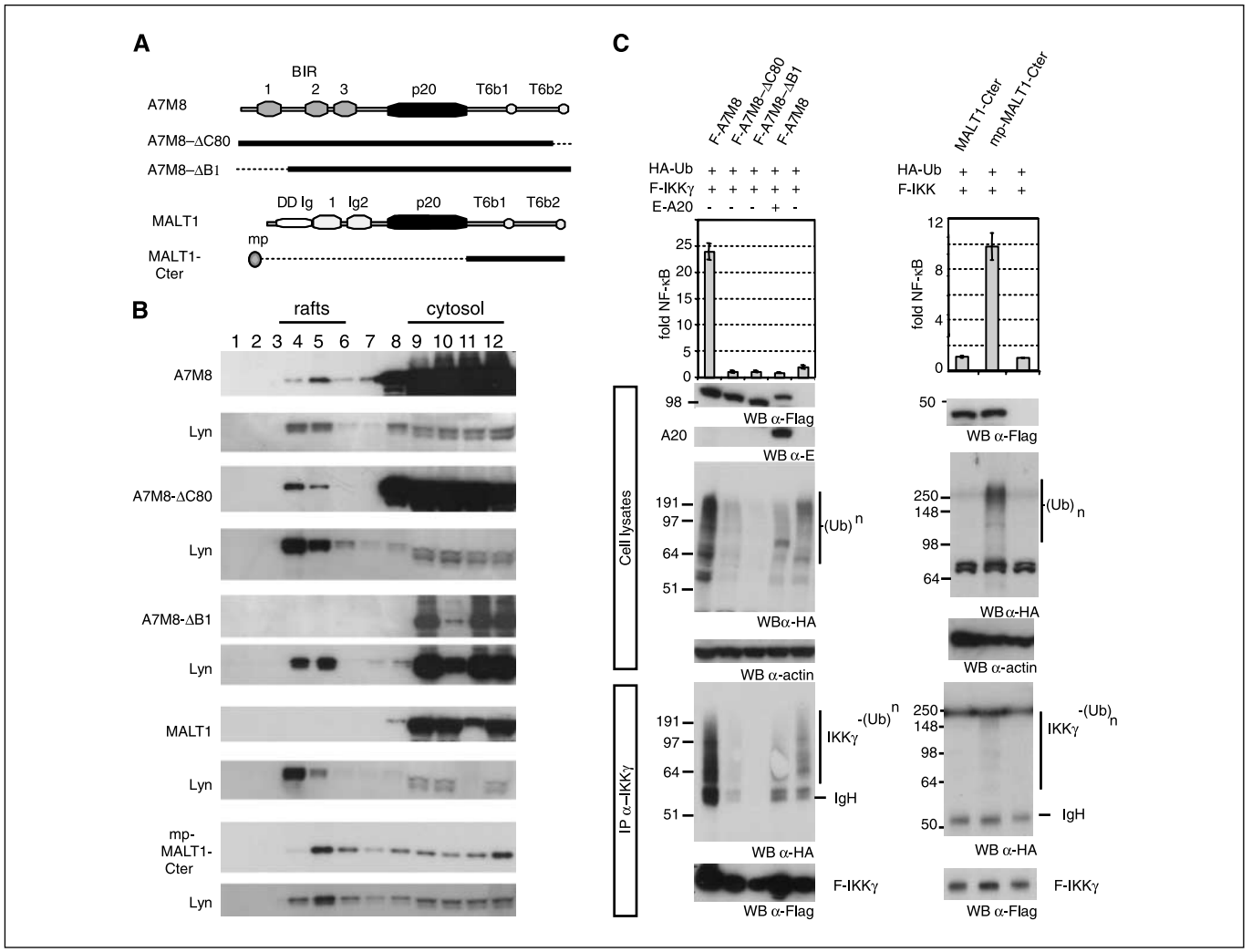

Figure 6. Raft association of the COOH terminal of MALT1 induces NF-κB activation. *A*, structural domains of the API2-MALT1 fusion variant A7M8 and MALT1 plus the domain content (*solid bars*) of the API2-MALT1 deletion constructs and of mp-MALT1-Cter. *MP,* myristoylation/palmitoylation motif of Lck. *B*, lysates of HEK293T cells transiently transfected with 4 μg of the indicated constructs were subjected to sucrose density gradient centrifugation, and fractions were immunoblotted with α-Flag and α-Lyn. *C*, HEK293T cells were transfected with a NF-κB-dependent luciferase reporter plasmid, an internal control plasmid carrying a *β-galactosidase* gene, 2 ng pcD-F-IKKγ, and 40 ng pcD-HA-Ub, together with empty vector (−) or 200 ng of the indicated constructs. Cell lysates were immunoblotted with α-Flag or α-HA antibodies and α-β-actin to show equal loading. α-IKKγ immunoprecipitates were immunoblotted with α-HA or α-Flag. Molecular weight standards are in kDa. NF-κB-dependent luciferase activity as fold induction of vector-transfected cells. *Columns,* mean of at least three independent experiments; *bars,* SD.

As the fusion protein is deficient for BCL10 nuclear export, the relative shortage of MALT1 might account for the observed nuclear retention of BCL10 in MALT lymphomas with t(11;18) (30). However, BCL10 staining in our API2-MALT1 transgenic mice and their WT littermates revealed a diffuse cytoplasmic BCL10 expression pattern in the B cells of the follicle mantle with only a few scattered B cells in between showing a nuclear staining. This observation indicates that besides MALT lymphoma development, also aberrant nuclear BCL10 expression requires more than the presence of the API2-MALT1 fusion transcript alone.

Despite these negative observations, it is of interest to note that AM31 transgenic mice displayed some morphologic differences in the development of the white pulp of the spleen compared with their equally old WT littermates. The most remarkable finding was an expansion of the follicle mantle with a well-developed marginal zone in transgenic mice compared with WT mice. A similar observation was made in BCL10 transgenic mice (32), with an overexpression of the BCL10 protein as is seen in t(1;14)(p22;q21)-associated MALT-type lymphomas. The morphologic observations of an expanded follicle mantle in the API2-MALT1 transgenic mice were confirmed by FACS analyses, which clearly showed an increase of $IgM^{high}IgD^{low}$ and $CD21^{high}CD23^{low}$ B cells corresponding to the marginal zone B-cell population, suggesting that the API2-MALT1 fusion favors the development of marginal zone B cells and/or promotes their proliferation or survival. In support for the first, the BCR signal-strength model hypothesizes that the T2 transitional B-cell population in the spleen will maturate to marginal zone B cells on weak BCR signals; intermediate signals are required for follicular B-cell development, whereas strong BCR signals drive B1 B-cell development (33). Expression of API2-MALT1 could influence this cell fate decision process by constitutively activating NF-κB, in this way providing a continuous weak BCR-like signal that can advance the cell fate decision point and direct it toward marginal zone B-cell differentiation before additional (stronger) BCR signals could affect this process.

Besides an effect on splenic marginal zone B cells, we observed reduced relative levels of B-cell precursors in the bone marrow and noticed that pre-B cells of API2-MALT1 transgenic mice fail to proliferate and form colonies in methylcellulose containing IL-7 (Fig. 4*D*). During B-cell development in the bone marrow, productive IgH rearrangement followed by pre-BCR assembly triggers progression to the precursor (pre-)B-cell stage, at which IL-7 alone is sufficient to provoke a limited number of cell divisions (34). On subsequent rearrangement of the light chain, IL-7-dependent proliferation of these B cells is constrained by an inhibitory signal initiated through antigen receptor assembly (35). This rearrangement of the light chain requires activation of the p50/p65 subunits of NF-κB, which is normally mediated by the pre-BCR (36). As API2-MALT1 expression is driven by the Eμ enhancer, which is already active in the earliest committed B lymphocyte progenitors (pre-pro-B cells) when D_H to J_H rearrangement first takes place (22), its expression might trigger or enhance NF-κB activation at the pre-pro-B-cell stage, resulting in the simultaneous rearrangement of the light and heavy chains. Premature expression of a functional BCR in that case constrains IL-7-dependent proliferation of pre-B cells and accelerates their maturation to naive B cells (IgM^{low}/IgD^{low}). The limited proliferation of pre-B cells then explains the reduced numbers of B cells in the bone marrow, whereas acceleration of their maturation might account for the increased relative number of naive B cells in the spleen of AM31 transgenic mice. The latter could furthermore explain the earlier development (at 5 weeks) of germinal centers in AM31 transgenic mice, most likely triggered by antigen stimulation due to the non-pathogen-free housing conditions. Finally, the normal spleen size representing normal lymphocyte numbers, in contrast to reduced proliferation of precursor B cells in the bone marrow, could be explained by the API2-MALT1-mediated effect on proliferation or survival of splenic B cells as shown in the *ex vivo* survival assay and can be attributed to the constitutive NF-κB activation as shown by enhanced polyubiquitination of IKKγ in splenic lymphocytes.

Recruitment of BCL10 (15) and MALT1 (16) to the lipid rafts at the TCR is essential for NF-κB activation. Immunofluorescence microscopic analyses of COS7 cells indicated that the API2-MALT1 fusion resides in the cytoplasm (37). We showed that the first BIR domain of API2 also determines raft association of the MALT1 portion of the fusion, which is sufficient to activate NF-κB signaling. Therefore, permanent raft association of API2-MALT1, as observed in splenic lymphocytes of AM31 transgenic mice, might, together with sustained expression of API2-MALT1 via NF-κB-mediated up-regulation of its own expression in t(11;18)-carrying MALT lymphomas (38), represent the mechanism to induce constitutive NF-κB activity resulting in increased B-cell survival and circumvent the necessity of antigen receptor stimulation. Indeed, also, in API2-MALT1 expressing BJAB cells, the fusion protein was associated with the lipid rafts, which coincided with increased NF-κB activity and resistance to Fas-induced apoptosis (17).

Polyubiquitination of IKKγ by TRAF6 plays a central role in the TCR pathway leading to NF-κB activation. MALT1 contains two potential TRAF6-binding sites in its COOH terminal (11), and BCL10-mediated dimerization of MALT1 activates the ligase activity of TRAF6 via oligomerization of its RING domain. Remarkably, a recent report suggested that the TRAF6-binding sites are not required for activation of NF-κB and attributed this role to a new COOH-terminal MALT1 domain that interacts with Ubc13 (12). In contrast, our experiments clearly underline the importance of the second TRAF6-binding site of MALT1 for NF-κB activation by A7M8. This discrepancy might be caused by the API2-MALT1 fusion variant used by us (A7M8) that does not contain the Ig-like domains of MALT1, which could account for the observed differences. The same group further reported that the first BIR domain of API2 mediates NF-κB activation via oligomerization of the API2-MALT1 fusion protein. Our results indicate that the first BIR domain is also involved in raft association of API2-MALT1, which is required for NF-κB activation. Possibly, raft localization facilitates the oligomerization of the fusion protein and its interaction with downstream signaling components, such as TRAF6, to induce polyubiquitination of IKKγ. In line with this hypothesis is our observation that the TRAF6-binding site mutant A7M8-ΔC80 resided in the lipid rafts although was defective for NF-κB activation.

In summary, we show that the specific expansion of splenic marginal zone B cells in API2-MALT1 transgenic mice and the increased survival of their B cells *ex vivo* are associated with enhanced polyubiquitination of IKKγ, and we identify permanent raft association of the fusion protein as a mechanism for constitutive NF-κB activation. Thus, the API2-MALT1 fusion protein contributes to MALT lymphoma development via constitutive NF-κB activation, and the generated transgenic mice will be valuable to analyze further the signaling events associated with API2-MALT1 expression.

Acknowledgments

Received 12/22/2005; revised 2/8/2006; accepted 3/9/2006.

Grant support: Belgische Federatie tegen Kanker grant SCIE2003-09 and Association for International Cancer Research grant 04-149 (P. Marynen) and Fonds voor Wetenschappelijk Onderzoek (FWO)-Vlaanderen "Krediet aan Navorsers" 1.5.145.04 (M. Baens) and grant G.0091.02 (S. Fevery). H. Noels and X. Sagaert are FWO-Vlaanderen aspirants, and A.D. Billiau is a FWO-Vlaanderen postdoctoraal onderzoeker.

The costs of publication of this article were defrayed in part by the payment of page charges. This article must therefore be hereby marked *advertisement* in accordance with 18 U.S.C. Section 1734 solely to indicate this fact.

We thank Anton Roebroek for the generation of the API2-MALT1 transgenic mice.

References

1. Dierlamm J, Baens M, Wlodarska I, et al. The apoptosis inhibitor gene API2 and a novel 18q gene, MLT, are recurrently rearranged in the t(11;18)(q21;q21) associated with mucosa-associated lymphoid tissue lymphomas. Blood 1999;93:3601–9.
2. Willis TG, Jadayel DM, Du MQ, et al. Bcl10 is involved in t(1;14)(p22;q32) of MALT B cell lymphoma and mutated in multiple tumor types. Cell 1999;96:35–45.
3. Zhang Q, Siebert R, Yan M, et al. Inactivating mutations and overexpression of BCL10, a caspase recruitment domain-containing gene, in MALT lymphoma with t(1;14)(p22;q32). Nat Genet 1999;22:63–8.
4. Streubel A, Lamprecht A, Dierlamm J, et al. t(14;18)(q32;q21) involving IGH and MALT1 is a frequent chromosomal aberration in MALT lymphoma. Blood 2003;101:2335–9.
5. Sanchez-Izquierdo D, Buchonnet G, Siebert R, et al. MALT1 is deregulated by both chromosomal translocation and amplification in B-cell non-Hodgkin lymphoma. Blood 2003;101:4539–46.
6. Ruland J, Duncan GS, Elia A, et al. Bcl10 is a positive regulator of antigen receptor-induced activation of NF-κB and neural tube closure. Cell 2001;104:33–42.
7. Ruland J, Duncan GS, Wakeham A, Mak TW. Differential requirement for Malt1 in T and B cell antigen receptor signaling. Immunity 2003;19:749–58.
8. Ruefli-Brasse AA, French DM, Dixit VM. Regulation of NF-κB-dependent lymphocyte activation and development by paracaspase. Science 2003;302:1581–4.
9. Uren GA, O'Rourke K, Aravind L, et al. Identification of paracaspases and metacaspases: two ancient families of caspase-like proteins, one of which plays a key role in MALT lymphoma. Mol Cell 2000;6:961–7.
10. Lucas PC, Yonezumi M, Inohara N, et al. Bcl10 and MALT1, independent targets of chromosomal translocation in MALT lymphoma, cooperate in a novel NF-κB signaling pathway. J Biol Chem 2001;276:19012–9.
11. Sun LJ, Deng L, Ea CK, Xia ZP, Chen ZJJ. The TRAF6 ubiquitin ligase and TAK1 kinase mediate IKK activation

by BCL10 and MALT1 in T lymphocytes. Mol Cell 2004; 14:289–301.
12. Zhou HL, Du MQ, Dixit VM. Constitutive NF-κB activation by the t(11;18)(q21;q21) product in MALT lymphoma is linked to deregulated ubiquitin ligase activity. Cancer Cell 2005;7:425–31.
13. Wang D, You Y, Case SM, et al. A requirement for CARMA1 in TCR-induced NF-κB activation. Nat Immunol 2002;3:830–5.
14. Gaide O, Favier B, Legler DF, et al. CARMA1 is a critical lipid raft-associated regulator of TCR-induced NF-κB activation. Nat Immunol 2002;3:836–43.
15. Wang D, Matsumoto R, You Y, et al. CD3/CD28 costimulation-induced NF-κB activation is mediated by recruitment of protein kinase C-θ, Bcl10, and IκB kinase β to the immunological synapse through CARMA1. Mol Cell Biol 2004;24:164–71.
16. Che TJ, You Y, Wang DH, Tanner MJ, Dixit VM, Lin X. MALT1/paracaspase is a signaling component downstream of CARMA1 and mediates T cell receptor-induced NF-κB activation. J Biol Chem 2004;279: 15870–6.
17. Ho L, Davis RE, Conne B, et al. MALT1 and the API2-MALT1 fusion act between CD40 and IKK and confer NF-κB-dependent proliferative advantage and resistance against FAS-induced cell death in B cells. Blood 2005; 105:2891–9.
18. Bodrug SE, Warner BJ, Bath ML, Lindeman GJ, Harris AW, Adams JM. Cyclin D1 transgene impedes lymphocyte maturation and collaborates in lymphomagenesis with the myc gene. EMBO J 1994;13:2124–30.
19. Brinster RL, Chen HY, Trumbauer M, Senear AW, Warren R, Palmiter RD. Somatic expression of herpes thymidine kinase in mice following injection of a fusion gene into eggs. Cell 1981;27:223–31.
20. Heyninck K, De Valck D, Vanden Berghe W, et al. The zinc finger protein A20 inhibits TNF-induced NF-κB-dependent gene expression by interfering with an RIP- or TRAF2-mediated transactivation signal and directly binds to a novel NF-κB-inhibiting protein ABIN. J Cell Biol 1999;145:1471–82.
21. Liu HX, Ye HT, Ruskone-Fourmestraux A, et al. T(11;18) is a marker for all stage gastric MALT lymphomas that will not respond to *H-pylori* eradication. Gastroenterology 2002;122:1286–94.
22. Li YS, Wasserman R, Hayakawa K, Hardy RR. Identification of the earliest B lineage stage in mouse bone marrow. Immunity 1996;5:527–35.
23. Ye H, Dogan A, Karran L, et al. BCL10 expression in normal and neoplastic lymphoid tissue. Nuclear localization in MALT lymphoma. Am J Pathol 2000;157:1147–54.
24. Liu HX, Ye HT, Dogan A, et al. T(11;18)(q21;q21) is associated with advanced mucosa-associated lymphoid tissue lymphoma that expresses nuclear BCL10. Blood 2001;98:1182–7.
25. Maes B, Demunter A, Peeters B, Wolf-Peeters C. *BCL10* mutation does not represent an important pathogenic mechanism in gastric MALT-type lymphoma, and the presence of the *API2-MLT* fusion is associated with aberrant nuclear BCL10 expression. Blood 2002;99:1398–404.
26. Ye H, Liu H, Raderer M, et al. High incidence of t(11;18)(q21;q21) in Helicobacter pylori-negative gastric MALT lymphoma. Blood 2003;101:2547–50.
27. Gugasyan R, Grumont R, Grossmann M, et al. Rel/NF-κB transcription factors: key mediators of B-cell activation. Immunol Rev 2000;176:134–40.
28. Cavalli F, Isaacson PG, Gascoyne RD, Zucca E. MALT lymphomas. Hematology (Am Soc Hematol Educ Program) 2001;241–58.
29. Strasser A, Harris AW, Cory S. Eμ-bcl-2 transgene facilitates spontaneous transformation of early pre-B and immunoglobulin-secreting cells but not T-cells. Oncogene 1993;8:1–9.
30. Nakagawa M, Hosokawa Y, Yonezumi M, et al. MALT1 contains nuclear export signals and regulates cytoplasmic localization of BCL10. Blood 2005;106: 4210–6.
31. Isaacson PG, Du MQ. MALT lymphoma: from morphology to molecules. Nat Rev Cancer 2004;4:644–53.
32. Zhang Q, Cui X, Sangster MY, et al. Selective hyperexpansion of marginal zone (MZ) B-cells in Eμ-BCL10 mice. Blood 2000;96:822A.
33. Pillai S, Cariappa A, Moran ST. Marginal zone B cells. Annu Rev Immunol 2005;23:161–96.
34. Namen AE, Schmierer AE, March CJ, et al. B cell precursor growth-promoting activity. Purification and characterization of a growth factor active on lymphocyte precursors. J Exp Med 1988;167:988–1002.
35. Smart FM, Venkitaraman AR. Inhibition of interleukin 7 receptor signaling by antigen receptor assembly. J Exp Med 2000;191:737–42.
36. Siebenlist U, Brown K, Claudio E. Control of lymphocyte development by nuclear factor-κB. Nat Rev Immunol 2005;5:435–45.
37. Izumiyama K, Nakagawa M, Yonezumi M, et al. Stability and subcellular localization of API2-MALT1 chimeric protein involved in t(11;18)(q21;q21) MALT lymphoma. Oncogene 2003;22:8085–92.
38. Hosokawa Y, Suzuki H, Nakagawa M, Lee TH, Seto M. API2-MALT1 fusion protein induces transcriptional activation of the API2 gene through NF-κB binding elements: evidence for a positive feed-back loop pathway resulting in unremitting NF-κB activation. Biochem Biophys Res Commun 2005;334:51–60.

Selective Expansion of Marginal Zone B Cells in Eμ -API2-MALT1 Mice Is Linked to Enhanced IκB Kinase γ Polyubiquitination

Mathijs Baens, Sabine Fevery, Xavier Sagaert, et al.

Cancer Res 2006;66:5270-5277.